Eur. Phys. J. Special Topics **227**, 2001–2012 (2019)

https://doi.org/10.1140/epjst/e2019-800052-2

THE EUROPEAN PHYSICAL JOURNAL SPECIAL TOPICS

Regular Article

Thermal and quantum decay of supercurrent in highly transparent weak links

Artem V. Galaktionov[1], Dmitry S. Golubev[2], and Andrei D. Zaikin[3,4,a]

[1] I.E. Tamm Department of Theoretical Physics, P.N. Lebedev Physical Institute, 119991 Moscow, Russia
[2] Low Temperature Laboratory, Department of Applied Physics, Aalto University, Espoo, Finland
[3] Institute of Nanotechnology, Karlsruhe Institute of Nanotechnology (KIT), 76021 Karlsruhe, Germany
[4] National Research University Higher School of Economics, 101000 Moscow, Russia

Received 13 April 2018 / Received in final form 13 June 2018
Published online 13 February 2019

Abstract. We analyze a trade-off between thermal activation (TA) and quantum tunneling in the problem of supercurrent decay in superconducting junctions with highly transparent barriers. In such systems – unlike in conventional tunnel junctions – the supercurrent decay is essentially influenced by low energy Andreev levels forming an intrinsic quantum dissipative environment for the Josephson particle. We evaluate the temperature dependent supercurrent decay rate $\Gamma(T)$ and elucidate a variety of different regimes for such a decay. We demonstrate that no classical-to-quantum crossover exists in the limit of fully transparent barriers, in which case quantum tunneling always prevails over TA.

1 Introduction

It is well known that both thermal and quantum fluctuations can fully suppress superconductivity in ultrasmall Josephson tunnel junctions [1]. This process can be viewed as a result of an escape of the Josephson "particle" with "coordinate" φ from its effective potential well due to either thermal activation (TA) or macroscopic quantum tunneling (MQT). The Josephson phase φ plays the role of a collective quantum variable that can also interact with other degrees of freedom forming an effective environment. This quantum environment can be treated phenomenologically as a set of harmonic oscillators [2–4] or microscopically [1,5] as electron sea in a disordered metal. Tracing out the environment degrees of freedom one arrives at the Feynman–Vernon influence functional (or effective action) describing quantum dissipation. More sophisticated versions of the influence functional [6,7] also account for Fermi statistics for electrons in a metal forming an effective environment "for themselves".

Dissipation can strongly affect MQT of the Josephson phase in superconducting tunnel junctions [3,4]. There dissipation at subgap energies can only occur extrinsically as no states with energies below the superconducting gap Δ exist in

[a] e-mail: andrei.zaikin@int.fzk.de

such systems. In contrast, subgap bound states (Andreev levels [8,9]) do occur in superconducting weak links with higher (non-tunnel) transmissions. Recently, we demonstrated [10] that such low energy Andreev states can form an *intrinsic* effective quantum dissipative environment for the Josephson phase φ which can strongly modify quantum dynamics of superconducting weak links with respect to that for tunnel junctions. For instance, MQT process of the Josephson phase φ acquires a number of novel features [10–12].

In this paper, we will further investigate both TA and MQT effects in highly transparent superconducting contacts. We will develop a detailed analysis of the temperature dependent supercurrent decay rate $\Gamma(T)$ influenced by intrinsic quantum dissipative environment formed by low energy Andreev levels. In particular, we will demonstrate that in the limit of fully transparent barriers quantum tunneling always prevails over TA.

2 Low energy Hamiltonian and effective action

Let us consider a short superconducting junction characterized by geometric capacitance C_0 and an arbitrary distribution of normal transmissions T_n among $\mathcal{N}$ transport channels. As long as fluctuations of the Josephson phase φ can be neglected the junction may conduct the supercurrent I_S described by the current-phase relation [13–15]

$$I_S(\varphi) = \frac{e\Delta^2 \sin\varphi}{2} \sum_n \frac{T_n}{\epsilon_n(\varphi)} \tanh \frac{\epsilon_n(\varphi)}{2T}, \tag{1}$$

where

$$\epsilon_n(\varphi) = \Delta\sqrt{1 - T_n \sin^2(\varphi/2)} \tag{2}$$

defines the energies of subgap Andreev bound states $\pm\epsilon_n(\varphi)$ inside the weak link. In the tunneling limit $T_n \ll 1$ equation (1) reduces to the standard dependence $I_S(\varphi) = I_C \sin\varphi$ with the critical current $I_C(T)$ defined by the Ambegaokar–Baratoff formula [16]. However, in contacts with higher transmissions $T_n \sim 1$ both the temperature dependence of the critical current $I_C(T)$ and the low temperature current-phase relation $I_S(\varphi)$ in equation (1) differ substantially from those for conventional tunnel barriers, as it was demonstrated experimentally in a variety of junctions including, e.g., junctions with carbon nanotubes [17–19], atomic point contacts [20,21], graphene-based weak links [22–24], high transparency Al/BiTe/Al double barrier heterostructures [25], InAs nanowire Josephson junctions [26–28], as well as both 2d and 3d topological insulators [29–31] where effective channel transmissions with values close to unity were reached.

In the presence of fluctuations of the phase φ one can work out a general effective action approach that holds at arbitrary transmission values T_n [32]. Unfortunately, this technique turns out to be rather involved. Simplifications occur if we assume that phase fluctuations remain sufficiently weak [33,34] in which case we can split the phase variable into constant and fluctuating parts $\varphi(t) = \chi + \phi(t)$ with $|\phi(t)| \ll 1$. It is possible to demonstrate that, provided both temperature T and typical phase fluctuation frequencies ω_ϕ remain sufficiently small, $T, \omega_\phi \ll \Delta$, our superconducting weak link is described by an effective Hamiltonian [10]

$$\hat{H} = -\frac{2e^2}{C}\frac{\partial^2}{\partial\phi^2} + U(\chi+\phi) + \sum_n \left[\frac{\hat{P}_n^2}{2M_n} + \frac{M_n\omega_n^2}{2}\left(Q_n - \frac{c_n\phi}{M_n\omega_n^2}\right)^2\right]. \tag{3}$$

The first two terms in the right-hand side of equation (3) describe the Josephson "particle" with effective "mass" $C/(2e)^2$ propagating in the potential

$$U(\varphi) = -2T\sum_n \ln\left[\cosh\frac{\epsilon_n(\varphi)}{2T}\right] - \frac{I\varphi}{2e}, \tag{4}$$

where the first term in the right-hand side defines the 2π-periodic potential and the second term produces a tilt due to the presence of a current bias I. Setting the derivative of the potential energy U in equation (4) with respect to the phase φ equal to zero, one arrives at the equation $I_S(\chi) = I$ fixing the equilibrium phase value χ.

The last term in equation (3) accounts for an effective environment formed by subgap Andreev levels. It consists of $\mathcal{N}$ harmonic oscillators with frequencies $\omega_n = 2\epsilon_n(\chi)$ coupled to the "particle coordinate" ϕ. The coupling constant values c_n are determined by the condition [10]

$$\frac{c_n^2}{M_n} \equiv \gamma_n = T_n^2(1-T_n)\frac{\Delta^4}{\epsilon_n(\chi)}\sin^4\frac{\chi}{2}\tanh\frac{\epsilon_n(\chi)}{2T}. \tag{5}$$

What remains is to include the effect of quasiparticles with overgap energies which in the limit $T, \omega_\phi \ll \Delta$ provide renormalization of the geometric capacitance C_0 [33]. Depending on the parameters this renormalization can be significant. For example, in the limit $1 - T_n \ll 1$ and $\pi - \chi \ll \pi$ we get [10]

$$C \simeq C_0 + e^2\mathcal{N}/(4\Delta). \tag{6}$$

Employing the effective Hamiltonian in equation (3) it is straightforward construct the grand partition function for our weak link $\mathcal{Z}$. Expressing $\mathcal{Z}$ in terms of the path integral over both ϕ and the oscillator coordinates Q_n and integrating out all Q_n-variables, we obtain

$$\mathcal{Z} = \mathrm{Sp}e^{-\beta\hat{H}} = \int \mathrm{D}\phi \exp\left(-S_{\mathrm{eff}}[\phi(\tau)]\right), \tag{7}$$

where here and below $\beta \equiv 1/T$,

$$S_{\mathrm{eff}} = \int_0^\beta d\tau\left[\frac{C\dot{\phi}^2}{8e^2} + U(\chi+\phi(\tau))\right] + \int_0^\beta d\tau_1\int_0^\beta d\tau_2 Y(\tau_1-\tau_2)\phi(\tau_1)\phi(\tau_2) \tag{8}$$

is the imaginary time effective action for our superconducting contact and

$$Y(\tau) = \sum_n \frac{\gamma_n}{8\epsilon_n}\left(\frac{\delta(\tau)}{\epsilon_n} - \frac{\cosh\left[2\epsilon_n\left(|\tau| - \frac{1}{2T}\right)\right]}{\sinh[\epsilon_n/T]}\right). \tag{9}$$

Expanding the kernel (9) in the Fourier series $Y(\tau) = T\sum_{\omega_m} Y_{\omega_m} e^{-i\omega_m\tau}$, we get

$$Y_{\omega_m}(\chi) = \sum_n \frac{\gamma_n(\chi)}{8\epsilon_n^2(\chi)}\frac{\omega_m^2}{\omega_m^2 + 4\epsilon_n^2(\chi)}, \quad \omega_m = 2\pi m T. \tag{10}$$

3 Decay rate

Provided the bias current value I gets sufficiently close to the critical current I_C the zero resistance state of our superconducting weak link becomes unstable and can decay into a resistive state implying that the phase variable φ overcomes the potential barrier $U(\varphi)$ due to either TA or MQT.

Following [10,11] below we will stick to the limit of large number of channels $\mathcal{N} \gg 1$ in our weak link and assume that all barrier transmissions have the same value $T_n = \mathcal{T}$ and, hence, $\epsilon_n(\chi) \equiv \epsilon(\chi)$, cf. equation (2). We also define the reflection coefficient $r = 1 - \mathcal{T} \ll 1$ and the parameter $q(T) = 1 - I/I_C(T) \ll 1$.

At $T \to 0$ the effective potential (4) reduces to a simple form

$$U(\varphi) = -I\varphi/2e - \mathcal{N}\Delta\sqrt{1 - \mathcal{T}\sin^2(\varphi/2)}. \tag{11}$$

For $q \ll \sqrt{r}$ equation (11) can be expanded in powers of ϕ around $\chi = \chi_c = \pi - \arccos[(1-\sqrt{r})^2/\mathcal{T}]$, where the phase value χ_c is defined by the equation $I_S(\chi_c) = I_C$. Dropping an unimportant constant we obtain

$$U(\chi_c + \phi) \simeq \frac{\Delta\mathcal{N}\nu}{2}\left[q\phi - \frac{\phi^3}{6}\right], \quad \nu = 1 - \sqrt{r}. \tag{12}$$

Observing a strong inequality $r \ll 1$, below we will set $\nu \simeq 1$. For $q \gtrsim \sqrt{r}$ the expansion (12) is no more sufficient, and the exact form of U (11) should be employed.

One of the important features of the problem under consideration is that at small enough values of r the potential energy $U(\varphi)$ (4) essentially depends on temperature. For example, at $r \to 0$ we obtain

$$U(\varphi) = -2T\mathcal{N}\ln\left[\cosh\frac{\Delta\cos(\varphi/2)}{2T}\right] - \frac{I\varphi}{2e}. \tag{13}$$

At $r > 0$ and high enough temperatures $\Delta r^{1/4} \ll T \ll \Delta$ we have $\chi_c = \pi - (2T/\Delta)W(2\Delta^2/T^2)$ (with $W(z)$ defined by the equation $W\exp(W) = z$) and the approximation (12) with $\nu = 1$ applies without any further restrictions.

Following the standard procedure [4,35,36] we define the supercurrent decay rate Γ as:

$$\begin{aligned} \Gamma &= -2\mathrm{Im}\,F, \quad T < T_0; \\ \Gamma &= -2\frac{\beta}{\beta_0}\,\mathrm{Im}\,F, \quad T > T_0, \end{aligned} \tag{14}$$

where $\beta_0 \equiv 1/T_0$ and $F = -T\ln\mathcal{Z}$ is the system free energy. For a detailed relation between the ImF-method to be employed here and its derivation based on the semi-classical multidimensional periodic-orbit-WKB approach covering the whole temperature range on a unified basis see, e.g., the work [37].

The quantum-to-classical crossover temperature T_0 is determined as [10,11]

$$T_0 = \frac{\Omega\left[\omega_0, \alpha, \epsilon^2(\chi_c)/\omega_0^2\right]}{2\pi}, \quad \alpha = \frac{\gamma(\chi_c)\mathcal{N}E_C}{2\epsilon^4(\chi_c)}, \tag{15}$$

$$\Omega\left[\omega_0, \alpha, \epsilon^2(\chi_c)/\omega_0^2\right] = \frac{\omega_0}{\sqrt{2}}\sqrt{\theta + \sqrt{\theta^2 + 16\frac{\epsilon^2(\chi_c)}{\omega_0^2}}}, \; \theta = 1 - (1+\alpha)\frac{4\epsilon^2(\chi_c)}{\omega_0^2},$$

where $E_C = e^2/2C$ is the junction charging energy and $\omega_0 = \sqrt{2e^2\Delta\mathcal{N}(2q)^{1/2}/C}$ is the plasma oscillation frequency near the bottom of the potential well. One should bear in mind that the arguments of the function Ω are also temperature dependent, i.e. equation (15) determines T_0 in an implicit form.

Provided the geometric capacitance C_0 is large we immediately recover the standard result [35] $T_0 = \omega_0/(2\pi)$. In the opposite limit of small geometric capacitance in equation (15) we may set $C = e^2\mathcal{N}/(4\Delta)$. Then it is straightforward to demonstrate that for any relation between the system parameters the crossover temperature T_0 obeys the condition [10,11]

$$\Delta(8q)^{1/4}r^{1/8}/\pi = T_0^{\min} \le T_0 \le T_0^{\max} = \Delta(8q)^{1/4}/\pi, \tag{16}$$

where $q = q(T_0)$. In the limit $T_0 \ll \Delta r^{1/4}/\pi$ and at small enough q we have $T_0 = T_0^{\min}$, whereas for $T_0 \gtrsim \Delta r^{1/4}/\pi$ the crossover temperature approaches the r-independent result $T_0 = T_0^{\max}$.

3.1 Arrhenius regime

Deep in the classical Arrhenius regime $T \gg T_0$ the decay rate Γ is given by the standard expression

$$\Gamma = \frac{\omega_0}{2\pi}\exp(-\beta U_0), \tag{17}$$

where $U_0 = U(\sqrt{2q}) - U(-\sqrt{2q}) = \Delta\mathcal{N}(2q)^{3/2}/3$ is the effective potential barrier and the phase values $\phi = \pm\sqrt{2q}$ correspond respectively to the maximum and minimum of the potential (12). As the temperature gets closer to T_0 quantum corrections to the classical activation result (17) become progressively more pronounced. In order to include the effect of quantum fluctuations we will follow the standard approach [4,38].

Let us denote the contributions to the partition function $\mathcal{Z}$ originating from the phase fluctuations near the potential minimum and maximum respectively as $\mathcal{Z}_0$ and $\mathcal{Z}_b$. In order to evaluate both these contributions let us express the function ϕ in the vicinity of $\phi = \pm\sqrt{2q}$ as

$$\phi = -\sqrt{2q} + \sum_{n=-\infty}^{\infty} X_n \exp(i\nu_n\tau), \quad \phi = \sqrt{2q} + \sum_{n=-\infty}^{\infty} Y_n \exp(i\nu_n\tau). \tag{18}$$

Then we get

$$S[X] = \frac{C\beta}{8e^2}\sum_{n=-\infty}^{\infty}\lambda_n^{(0)}X_nX_{-n}, \quad \lambda_n^{(0)} = \nu_n^2 + \omega_0^2 + \alpha\frac{4\epsilon^2(\chi_c)\nu_n^2}{4\epsilon^2(\chi_c)+\nu_n^2} \tag{19}$$

and

$$S[Y] = \frac{C\beta}{8e^2}\sum_{n=-\infty}^{\infty}\lambda_n^{(b)}Y_nY_{-n}, \quad \lambda_n^{(b)} = \nu_n^2 - \omega_0^2 + \alpha\frac{4\epsilon^2(\chi_c)\nu_n^2}{4\epsilon^2(\chi_c)+\nu_n^2}. \tag{20}$$

As usually, the eigenvalue $\lambda_0^{(b)}$ is found negative which signals instability and results in the imaginary part of $\mathcal{Z}_b$ which can be established with the aid of a standard

analytic continuation procedure [4]. Combining the second equation (14) with

$$\mathrm{Im}\, F = -T\frac{\mathrm{Im}\, \mathcal{Z}_b}{\mathcal{Z}_0} \tag{21}$$

and evaluating $\mathrm{Im}\, F$, at $T > T_0$ we obtain

$$\Gamma = T_0 c_{qm} \exp(-\beta U_0), \tag{22}$$

where

$$c_{qm} \equiv \prod_{n=1}^{\infty} \frac{\lambda_n^{(0)}}{\lambda_n^{(b)}} = \frac{\sinh(\pi\lambda_+^+)\sinh(\pi\lambda_-^+)}{\sinh(\pi\lambda_+^-)\sin(\pi\lambda_-^-)}, \tag{23}$$

$$\lambda_\pm^+ = \sqrt{p_+ \pm \sqrt{p_+^2 - p^2}}, \quad \lambda_\pm^- = \sqrt{\pm p_- + \sqrt{p_-^2 + p^2}},$$

$$p_\pm = \frac{1+\alpha}{2\pi^2 T^2}\left[\epsilon^2(\chi_c) \pm (\omega_0/2)^2\right], \quad p = \frac{\epsilon(\chi_c)\omega_0}{2\pi^2 T^2}.$$

In the weak coupling limit of small α and for $\omega_0 \neq 2\epsilon(\chi_c)$ from equations (22), (23) we get

$$\Gamma = \frac{\omega_0}{2\pi}\left(1 - \frac{\alpha}{2}\frac{4\epsilon^2(\chi_c)}{\omega_0^2 + 4\epsilon^2(\chi_c)}\right) \tag{24}$$

$$\times \frac{\sinh\left[\frac{\beta\omega_0}{2}\left(1 + \frac{\alpha}{2}\frac{4\epsilon^2(\chi_c)}{\omega_0^2 - 4\epsilon^2(\chi_c)}\right)\right]\sinh\left[\beta\epsilon(\chi_c)\left(1 - \frac{\alpha}{2}\frac{4\epsilon^2(\chi_c)}{\omega_0^2 - 4\epsilon^2(\chi_c)}\right)\right]}{\sin\left[\frac{\beta\omega_0}{2}\left(1 - \frac{\alpha}{2}\frac{4\epsilon^2(\chi_c)}{\omega_0^2 + 4\epsilon^2(\chi_c)}\right)\right]\sinh\left[\beta\epsilon(\chi_c)\left(1 + \frac{\alpha}{2}\frac{4\epsilon^2(\chi_c)}{\omega_0^2 + 4\epsilon^2(\chi_c)}\right)\right]} \exp(-\beta U_0),$$

whereas in the adiabatic limit $\omega_0 \ll 2\epsilon(\chi_c)$ one finds

$$\Gamma = \frac{\omega_0}{2\pi\sqrt{1+\alpha}}\frac{\sinh\left(\frac{\beta\omega_0}{2\sqrt{1+\alpha}}\right)}{\sin\left(\frac{\beta\omega_0}{2\sqrt{1+\alpha}}\right)}\exp(-\beta U_0). \tag{25}$$

In the limit $\alpha \to 0$ both expressions (24) and (25) reduce to the standard result for the decay rate in the absence of dissipation [4].

3.2 Crossover regime

Let us note that the eigenvalue $\lambda_1^{(b)}$ vanishes at $T = T_0$ as $\lambda_1^{(b)} \propto (T - T_0)$. This observation implies that at temperatures in the immediate vicinity of T_0 it is necessary to also include higher orders in $Y_{\pm 1}$ in the expansion (20). Expressing the potential energy U near $\phi = \sqrt{2q}$ in the form

$$U = U_b - \frac{\omega_0^2}{16E_C}\left(\phi - \sqrt{2q}\right)^2 - \frac{\omega_0^2}{48E_C\sqrt{2q}}\left(\phi - \sqrt{2q}\right)^3, \tag{26}$$

at $T > T_0$ we get

$$S[Y] = \beta U_b + \frac{C\beta}{8e^2} \sum_{n=-\infty}^{\infty} \left(\lambda_n^{(b)} Y_n Y_{-n} - \frac{\omega_0^2}{\sqrt{2q}} \left(Y_{-2} Y_1^2 + Y_2 Y_{-1}^2 + 2 Y_0 Y_{-1} Y_1 \right) \right). \quad (27)$$

After integrating over Y_0 and $Y_{\pm n}$ with $n \geq 2$ the contribution to the effective action from the remaining modes becomes

$$\Delta S_1^{(b)} = \frac{C\beta}{8e^2} \left(2\lambda_1^{(b)} Y_1 Y_{-1} + B_4 Y_1^2 Y_{-1}^2 \right), \quad B_4 = \frac{\omega_0^2}{2q} \left(1 - \frac{\omega_0^2}{2\lambda_2^{(b)}} \right). \quad (28)$$

The result (28) implies that in order to recover the correct expression for Γ in the crossover region the term $1/\lambda_1^{(b)}$ in equation (22) should be replaced by the combination

$$\left(\frac{\pi C\beta}{8e^2 B_4} \right)^{1/2} \mathrm{erfc} \left[\lambda_1^{(b)} \left(\frac{C\beta}{8e^2 B_4} \right)^{1/2} \right] \exp \left[\lambda_1^{(b)2} \frac{C\beta}{8e^2 B_4} \right], \quad (29)$$

where $\mathrm{erfc}(x) \equiv \frac{2}{\sqrt{\pi}} \int_x^\infty dy \exp(-y^2)$ is the complementary error function. As a result we obtain

$$\Gamma = T_0 \sqrt{\pi} z \, \mathrm{erfc}(z) \exp(z^2) c_{qm} \exp(-\beta U_0), \quad (30)$$

where

$$z = \lambda_1^{(b)} \left(\frac{C\beta}{8e^2 B_4} \right)^{1/2}. \quad (31)$$

Making use of the property $\lim_{z\to\infty} \sqrt{\pi} z \, \mathrm{erfc}(z) \exp(z^2) = 1$, at high temperatures we again recover equation (22) that holds in the Arrhenius regime.

Note that while deriving the result (30) we always implied $T > T_0$. Analogous derivation can also be worked out for $T < T_0$ [4] which leads to the same result. The dependence of the decay rate Γ on temperature in the crossover region is illustrated in Figure 1.

3.3 Quantum tunneling

Let us finally address the MQT regime $T < T_0$. In references [10,11], we demonstrated that – depending on the barrier transmission – in the limit $T \to 0$ the supercurrent decay can be described by three different regimes: (i) weak intrinsic dissipation, (ii) strong intrinsic dissipation and (iii) strong capacitance renormalization. The regime (i) sets in for $q \gg \sqrt{r}$ and is characterized by weak coupling between the fluctuating phase ϕ and the effective bath of Andreev oscillators. In this case, MQT process occurs in the effective potential (11) and is weakly affected by intrinsic dissipation. For $q \lesssim \sqrt{r}$ coupling to Andreev oscillators become stronger and we obtain

$$\Gamma \simeq 6\sqrt{6U_0\tilde{\omega}_0/\pi} \exp[-36U_0/(5\tilde{\omega}_0)], \quad (32)$$

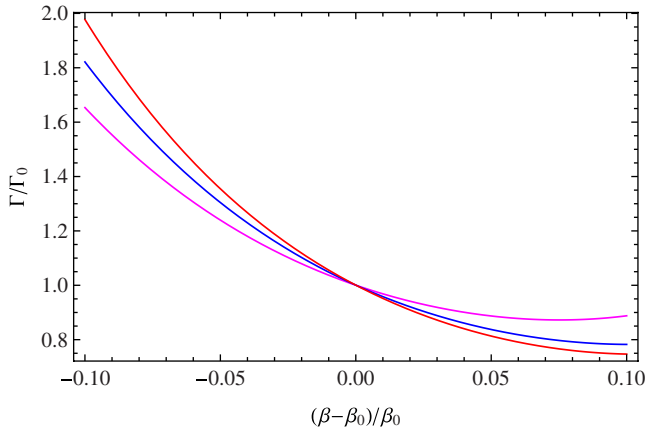

Fig. 1. Temperature dependence of the decay rate Γ (normalized to its value Γ_0 at $T = T_0$) in the vicinity of the crossover. The system parameters are set to be $(\pi/3)(\omega_0^2 q/\Omega E_C) = 15$ and $4\epsilon^2(\chi_c)/\omega_0^2 = 1$. The curves are plotted for $\alpha = 5$, 2 and 0.5 (magenta, blue and red, respectively). The corresponding values of Ω are $0.44\omega_0$, $0.64\omega_0$ and $0.88\omega_0$.

where $\tilde{\omega}_0 \simeq \omega_0$ for $C \simeq C_0$ and [10,11]

$$\tilde{\omega}_0 = 2\Delta\sqrt{\frac{Z}{2} + \sqrt{\frac{Z^2}{4} + \sqrt{8qr}}}, \quad Z = \sqrt{8q} - \sqrt{r} - r^{1/4}, \tag{33}$$

in the opposite limit of vanishing geometric capacitance C_0, i.e. for $C \simeq e^2\mathcal{N}/(4\Delta)$. In the latter limit, the strong dissipation regime (ii) takes place for $\sqrt{r} \gtrsim q > q_c = \sqrt{r}/32 + (r^{3/4} + r)/8$, while at $q < q_c$ the adiabatic regime (iii) of strong capacitance renormalization with $C^* = C + e^2\mathcal{N}/(4\Delta r^{1/4})$ sets in.

In order to determine the temperature dependence of Γ one should bear in mind that in weak links with small values of r the critical current $I_C(T)$ essentially depends on temperature also at $T \ll \Delta$, as it is illustrated, e.g., in Figure 2 (left panel). Accordingly, the MQT rate $\Gamma(T)$ increases with temperature because $q(T)$ decreases with increasing T and, hence, the potential barrier $U_0 \propto q^{3/2}$ becomes lower. Extra temperature dependence could occur due to coupling to Andreev oscillators provided T exceeds the interlevel distance $2\epsilon(\chi_c) = 2\Delta r^{1/4}$ for these oscillators. Obviously, this latter mechanism can be totally ignored at least as long as $T_0^{\max} < 2\Delta r^{1/4}$, i.e. for $q(T) < 2\pi^4 r$. In this case, the result (32) with $q = q(T)$ remains applicable at any $T < T_0$.

On the other hand, following the same line of reasoning one could conclude that for $T_0^{\min} > 2\Delta r^{1/4}$ (implying $\sqrt{r}/q(T) < 1/(2\pi^4) \ll 1$) temperature effects originating from the Andreev bath could possibly be expected. Note, however, that the above condition simultaneously implies very weak coupling between ϕ and Andreev oscillators. Hence, in this regime the bath effects can be disregarded as well and the temperature dependence of the MQT rate is determined solely by the potential profile $U(\varphi)$ that now changes with T, see, e.g., equation (13) and also Figure 2 (right panel).

In order to investigate this dependence below we set $r \to 0$. In this case, the phase variable ϕ is completely decoupled from Andreev oscillators and, hence, the quantum tunneling rate Γ can be evaluated by means of the standard semiclassical methods of quantum mechanics.

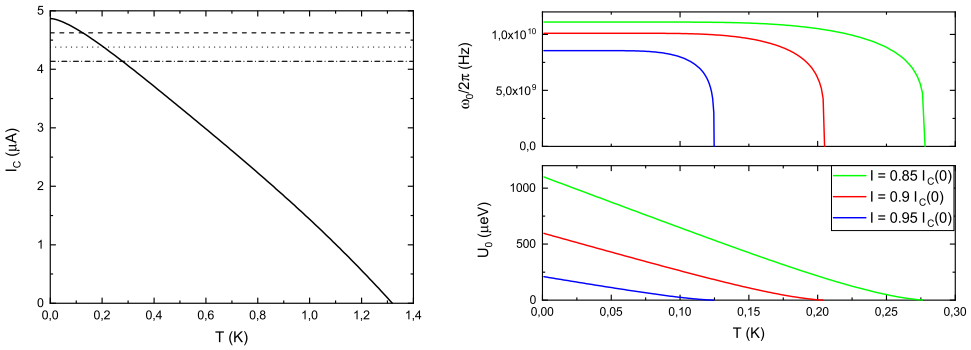

Fig. 2. Left panel: critical current $I_C(T)$ versus temperature (solid line) for a weak link with $r \to 0$. Horizontal lines correspond to bias current values $I = 0.85I_C(0)$, $0.9I_C(0)$ and $0.95I_C(0)$ (indicated respectively by dashed-dotted, dotted and dashed lines). Right panel: temperature dependence for both plasma frequency ω_0 and potential barrier U_0 for three bias current values. All curves correspond to the following parameters: $\mathcal{N} = 100$, $\Delta = 200\,\mu$eV, $E_C = 0.1\,\mu$eV and $T_C = 1.32\,$K.

To begin with, we determine the energy levels E_n in the potential well $U(\varphi)$. This task can be accomplished with the aid of the usual Bohr–Sommerfeld quantization rule:

$$\int_{\varphi_1(E_n)}^{\varphi_2(E_n)} d\varphi \frac{\sqrt{E_n - U(\varphi)}}{2\sqrt{E_C}} = \pi\left(n + \frac{1}{2}\right). \tag{34}$$

Here, $\varphi_1(E)$ and $\varphi_2(E)$ are two different solutions of the equation $E = U(\varphi)$, as it is illustrated in Figure 3 (left panel).

As a next step, we evaluate the quantum mechanical tunneling rate for the particle with energy E_n according to the standard formula

$$\Gamma_n = \frac{\omega_0}{2\pi} \exp\left[-\frac{1}{\sqrt{E_C}} \int_{\varphi_2(E_n)}^{\varphi_3(E_n)} \sqrt{U(\varphi) - E_n}\right], \tag{35}$$

where $\varphi_3(E_n)$ is the third solution of the equation $E_n = U(\varphi)$, see Figure 3 (left panel). The total equilibrium escape rate of the particle from the potential well can then be determined as [39]

$$\Gamma(T) = \sum_{n=0}^{N} P_n \Gamma_n, \quad P_n = \frac{e^{-E_n/T}}{\sum_{n'=0}^{N} e^{-E_{n'}/T}}. \tag{36}$$

Here, $N = N(I,T)$ is the total number of energy levels in the potential well. At sufficiently high temperatures $T \gg \omega_0/2\pi$ this expression approaches the classical TA formula (17), where now both values ω_0 and U_0 essentially depend on temperature, see Figure 2 (right panel).

The total escape rate (36) was evaluated numerically. The corresponding results are displayed in Figure 3 (right panel) demonstrating that no quantum-to-classical crossover exists in the fully transparent barrier limit $r \to 0$. This observation requires a comment.

It is well known [4,35] that the crossover between TA and MQT regimes always takes place, e.g., in Josephson tunnel barriers both with and without dissipation. The

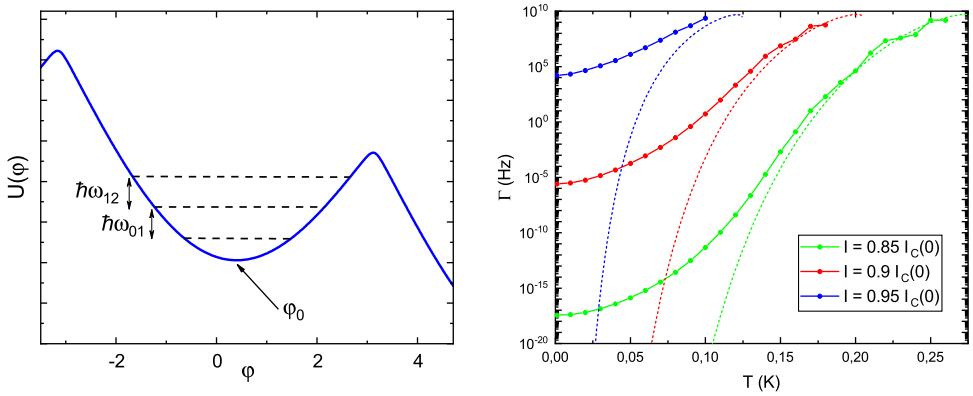

Fig. 3. Left panel: the effective potential profile $U(\varphi)$ at $T = 0$ and the energy levels in the potential well. Right panel: decay rate Γ versus temperature for three values of the bias current: $I = 0.85I_C(0)$ (green), $I = 0.9I_C(0)$ (red) and $I = 0.95I_C(0)$ (blue). Solid lines with symbols indicate the total decay rate (36). Thermal activation escape rate (17) (dashed lines) is presented for comparison. Here, the system parameters are set to be $N_{\rm ch} = 100$, $\Delta = 200\,\mu$eV and $E_C = 0.1\,\mu$eV.

physical nature of this crossover is obvious: the classical TA rate (17) (dominating the decay at higher T) decreases exponentially with temperature and eventually (at $T < T_0$) becomes lower than the MQT rate which remains non-zero down to $T = 0$. In other words, at $T < T_0$ the system favors quantum tunneling under the barrier whereas at $T > T_0$ the classical Arrhenius decay mechanism takes over, as it is already discussed above in Sections 3.1 and 3.2.

Note that, while this scenario applies for a "quadratic+qubic" potential (12), it may not work for some other potential profiles. For instance, earlier it was already demonstrated [40,41] that in the case of a non-quasiclassical potential of the type "quadratic+linear" and at any relevant temperature quantum tunneling prevails over TA and no quantum-to-classical crossover exists at all. Our results in Figure 3 (right panel) indicate that a similar situation occurs here in the full transmission limit $r \to 0$. Indeed, we observe that at all relevant T the supercurrent decays quantum mechanically with the rate $\Gamma(T)$ which remains bigger than the classical TA one (17) and gradually approaches the latter only in the high temperature limit. In other words, in the case of the potential (13) the system always "prefers" to tunnel under the barrier rather than to overcome it classically. In a way this behavior is understandable, since the overall shape of the potential energy (13) resembles that investigated in [40,41], in particular at sufficiently low T, cf. Figure 3 (left panel). At the same time, the situation considered here is quite different because of a strong dependence of the potential profile $U(\varphi)$ (13) on temperature which does not exist in the model [40,41]. More detailed analysis of this issue will be published elsewhere.

This work was supported in part by RFBR Grant No. 18-02-00586.

Author contribution statement

The authors declare that each of the three authors equally contributed to both the scientific contents and writing of this manuscript.

References

1. G. Schön, A.D. Zaikin, Phys. Rep. **198**, 237 (1990)
2. R.P. Feynman, A.R. Hibbs, *Quantum Mechanics and Path Integrals* (McGraw Hill, NY, 1965)
3. A.O. Caldeira, A.J. Leggett, Ann. Phys. **149**, 374 (1983)
4. U. Weiss, *Quantum Dissipative Systems* (World Scientific, Singapore, 2008)
5. V. Ambegaokar, U. Eckern, G. Schön, Phys. Rev. Lett. **48**, 1745 (1982)
6. D.S. Golubev, A.D. Zaikin, Physica B **255**, 164 (1998)
7. D.S. Golubev, A.D. Zaikin, G. Schön, J. Low Temp. Phys. **126**, 1355 (2002)
8. A.F. Andreev, Sov. Phys. JETP **22**, 455 (1966)
9. I.O. Kulik, Sov. Phys. JETP **30**, 944 (1970)
10. A.V. Galaktionov, D.S. Golubev, A.D. Zaikin, Phys. Rev. B **96**, 134509 (2017)
11. A.V. Galaktionov, D.S. Golubev, A.D. Zaikin, J. Supercond. Nov. Magn. **31**, 715 (2018)
12. D.S. Golubev, A.D. Zaikin, IEEE Trans. Appl. Supercond. **28**, 1700305 (2018)
13. I.O. Kulik, A.N. Omel'yanchuk, Sov. J. Low Temp. Phys. **4**, 142 (1978)
14. W. Haberkorn, H. Knauer, J. Richter, Phys. Status Solidi (A) **47**, K161 (1978)
15. C.W.J. Beenakker, Phys. Rev. Lett. **67**, 3836 (1991)
16. V. Ambegaokar, A. Baratoff, Phys. Rev. Lett. **10**, 486 (1963)
17. W. Liang, M. Bockrath, D. Bozovic, J.H. Hafner, M. Tinkham, H. Park, Nature **411**, 665 (2001)
18. P. Jarillo-Herrero, J.A. van Dam, L.P. Kouwenhoven, Nature **439**, 953 (2006)
19. J.-D. Pillet, C.H.L. Quay, P. Morfin, C. Bena, A. Levy Yeyati, P. Joyez, Nat. Phys. **6**, 965 (2010)
20. M.L. Della Rocca, M. Chauvin, B. Huard, H. Pothier, D. Esteve, C. Urbina, Phys. Rev. Lett. **99**, 127005 (2007)
21. C. Janvier, L. Tosi, L. Bretheau, C.O. Girit, M. Stern, P. Bertet, P. Joyez, D. Vion, D. Esteve, M.F. Goffman, H. Pothier, C. Urbina, Science **349**, 1199 (2015)
22. G.H. Lee, S. Kim, S.-H. Jhi, H.-J. Lee, Nat. Commun. **6**, 6181 (2015)
23. V.E. Calado, S. Goswami, G. Nanda, M. Diez, A.R. Akhmerov, K. Watanabe, T. Taniguchi, T.M. Klapwijk, L.M.K. Vandersypen, Nat. Nanotechnol. **10**, 761 (2015)
24. G. Nanda, J.L. Aguilera-Servin, P. Rakyta, A. Kormanyos, R. Kleiner, D. Koelle, K. Watanabe, T. Taniguchi, L.M.K. Vandersypen, S. Goswami, Nano Lett. **17**, 3396 (2017)
25. L. Galetti, S. Charpentier, Y. Song, D. Golubev, S.M. Wang, T. Bauch, F. Lombardi, IEEE Trans. Appl. Supercond. **27**, 1800404 (2017)
26. S. Abay, D. Persson, H. Nilsson, F. Wu, H.Q. Xu, M. Fogelström, V. Shumeiko, P. Delsing, Phys. Rev. B **89**, 214508 (2014)
27. E.M. Spanton, M. Deng, S. Vaitiekenas, P. Krogstrup, J. Nygard, C.M. Marcus, K.A. Moler, Nat. Phys. **13**, 1177 (2017)
28. M. Hays, G. de Lange, K. Serniak, D.J. van Woerkom, D. Bouman, P. Krogstrup, J. Nygard, A. Geresdi, M.H. Devoret, Phys. Rev. Lett. **121**, 047001 (2018)
29. I. Sochnikov, L. Maier, C.A. Watson, J.R. Kirtley, C. Gould, G. Tkachov, E.M. Hankiewicz, C. Brüne, H. Buhmann, L.W. Molenkamp, K.A. Moler, Phys. Rev. Lett. **114**, 066801 (2015)
30. M. Veldhorst, M. Snelder, M. Hoek, T. Gang, V.K. Guduru, X.L. Wang, U. Zeitler, W.G. van der Wiel, A.A. Golubov, H. Hilgenkamp, A. Brinkman, Nat. Mater. **11**, 417 (2012)
31. S. Charpentier, L. Galletti, G. Kunakova, R. Arpaia, Y. Song, R. Baghdadi, S.M. Wang, A. Kalaboukhov, E. Olsson, F. Tafuri, D. Golubev, J. Linder, T. Bauch, F. Lombardi, Nat. Commun. **8**, 2019 (2017)
32. A.D. Zaikin, Physica B **203**, 255 (1994)
33. A.V. Galaktionov, A.D. Zaikin, Phys. Rev. B **82**, 184520 (2010)
34. A.V. Galaktionov, A.D. Zaikin, Phys. Rev. B **92**, 214511 (2015)
35. I. Affleck, Phys. Rev. Lett. **46**, 388 (1981)
36. P. Hänggi, P. Talkner, M. Borkovec, Rev. Mod. Phys. **62**, 251 (1990)
37. P. Hänggi, W. Hontscha, Ber. Bunsenges. Phys. Chem. **95**, 379 (1991)

38. S. Kawabata, T. Bauch, T. Kato, Phys. Rev. B **80**, 174513 (2009)
39. D.A. Gorokhov, G. Blatter, Phys. Rev. B **56**, 3130 (1997)
40. A.D. Zaikin, S.V. Panyukov, Zh. Eksp. Teor. Fiz. **89**, 1890 (1985) [Sov. Phys. JETP **62**, 1091 (1985)]
41. A.D. Zaikin, I.N. Kosarev, S.V. Panyukov, Soviet Physics Lebedev Institute Reports N9, 25, 1987